

View Angle Tilting in Echo Planar Imaging for Distortion Correction

S. Ahn¹, and X. Hu¹

¹Biomedical Engineering, Georgia Institute of Technology and Emory University, Atlanta, GA, United States

INTRODUCTION

Geometric distortion caused by field inhomogeneity along the phase-encode (PE) direction is one of the most prominent artifacts due to a relatively low effective bandwidth in echo planar imaging (EPI). View angle tilting (VAT) technique [1] has been used for many applications to correct distortion in the readout (RO) direction in spin echo (SE) imaging. Recently, the possibility of extension of the VAT to EPI was briefly mentioned [2]. This work describes a method for correcting in-plane image distortion along the PE direction using the VAT technique in spin-echo EPI (SE-EPI). SE-EPI with VAT utilizes the addition of the VAT gradient blips along the slice-select (SS) direction, concurrently applied with the PE gradient blips, producing an additional phase. This phase offsets an unwanted phase accumulation caused by field inhomogeneity, resulting in the correction of image distortion along the PE direction.

METHODS AND MATERIALS

VAT technique was applied to address image distortion along the PE direction in a single-shot SE-EPI. When only considering image distortion along the PE direction and ignoring spin relaxation effects, the EPI signal can be expressed as

$$s(t_m, t_n) = \iiint_{x,y,z} \rho(x,y,z) \exp(-j\gamma \Delta B(x,y) n T_{\text{exp}}) \exp[-j\gamma (m G_x \Delta t_x x + n G_y t_b y)] dx dy dz, \text{ where } \rho(x,y,z) \text{ is spin density, } \gamma \text{ is the gyromagnetic ratio in radian} \cdot \text{sec}^{-1}$$

¹Tesla⁻¹, T_{exp} is the echo spacing, t_b is the duration of the PE gradient blip, $\Delta z(x,y)$ is the position displacement due to field inhomogeneity along the SS direction given by $\Delta z(x,y) = -\Delta B(x,y)/G_z$, G_z is the SS gradient, Δ_s is a slice thickness, and m and n are k-space indices along RO and PE directions, respectively. By reformulating using $z = z' - B(x,y)/G_z$ and by adding the VAT gradient ($G_{\text{vat}} = G_z T_{\text{exp}} / t_b$) along the SS direction concurrently with the PE gradient (Fig. 1), the above equation can be rewritten as

$$s(t_m, t_n) = \iiint_{x,y} \rho(x,y,z_0 - \frac{\Delta B(x,y)}{G_z}) \exp(-j\gamma n G_z T_{\text{exp}} z') \exp(j\gamma \frac{\Delta B(x,y) T_{\text{exp}}}{G_z t_b} n G_y t_b) \exp\{-j\gamma [m G_x \Delta t_x x + (y + \frac{\Delta B(x,y) T_{\text{exp}}}{G_z t_b}) n G_y t_b]\} dx dy dz'$$

$$= \iint_{x,y} \rho(x,y,z_0 - \frac{\Delta B(x,y)}{G_z}) \exp\{-j\gamma [m G_x \Delta t_x x + n G_y t_b y]\} dx dy \cdot \int_{\Delta_s} \exp(-j\gamma n G_z T_{\text{exp}} z') dz' = \iint_{x,y} \rho(x,y,z_0 - \frac{\Delta B(x,y)}{G_z}) \exp\{-j\gamma [m G_x \Delta t_x x + n G_y t_b y]\} dx dy \cdot \Delta_s \cdot \text{sinc}(\gamma n \Delta_s G_z T_{\text{exp}})$$

, where an optimal tilting angle is found to be $\tan(\theta) = G_{\text{vat}} / G_y = G_z T_{\text{exp}} / (G_y t_b)$. Spin density was assumed only dependent on a position (x,y) with z_0 being a constant value at each coordinate (x,y) in deriving the above equation. This relationship yields distortion correction along the PE direction with some residual phase which causes image blurring. Since the tilting angle in EPI is usually high, VAT was performed in combination with parallel imaging (acceleration factor R= 4).

All experiments were performed on a 3 T scanner (TRIO, Siemens Medical Solutions, Malvern, PA) using a body coil for transmission and a 12-channel head coil. SE-EPI was performed on a phantom and human brains with 2.7x2.7x5 mm resolution, 2520 Hz/pixel receiver bandwidth, GRAPPA (R= 4) and VAT ($\theta = 41.4^\circ$) for the phantom and 3.4x3.4x5 mm resolution, 3126 Hz/pixel bandwidth, GRAPPA (R= 4) and VAT($\theta = 44.6^\circ$) in vivo.

RESULTS AND DISCUSSIONS

Fig. 2 shows air (lower circle) and oil (upper circle) tubes submerged in water doped with Gd-DTPA. There show significant distortion and chemical shift artifact (indicated by arrow and arrow head in Fig. 2a) due to water-air and water-oil interface. Using parallel imaging, distortion and chemical shift were reduced (Fig. 2b). Correction of both artifacts could be appreciated with VAT imaging (Fig. 2c). However, severe image blurring occurred as expected from the theory. When VAT is combined with parallel imaging, both artifacts were effectively corrected for a quality image (Fig. 2d). Fig. 3 shows in vivo images of two human brain regions, medial temporal region near ear canal and orbitofrontal cortex (OFC) both of which typically experience field inhomogeneity due to air-tissue interface. VAT images (Fig. 3c, f) show distortion correction (indicated by circle and arrow) compared to both non-parallel (Fig. 3a, d) and parallel imaging (Fig. 3b, e). Distortion correction using the VAT technique is based on the assumption of homogeneous field across the slice which is not always the case in vivo. Therefore, in vivo EPI VAT imaging may not always provide the optimal correction of distortion, which depends on anatomical regions and slice orientation.

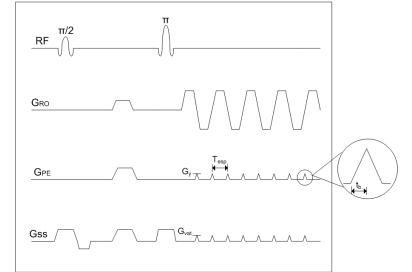


Figure 1. Pulse sequence diagram of SE-EPI with VAT.

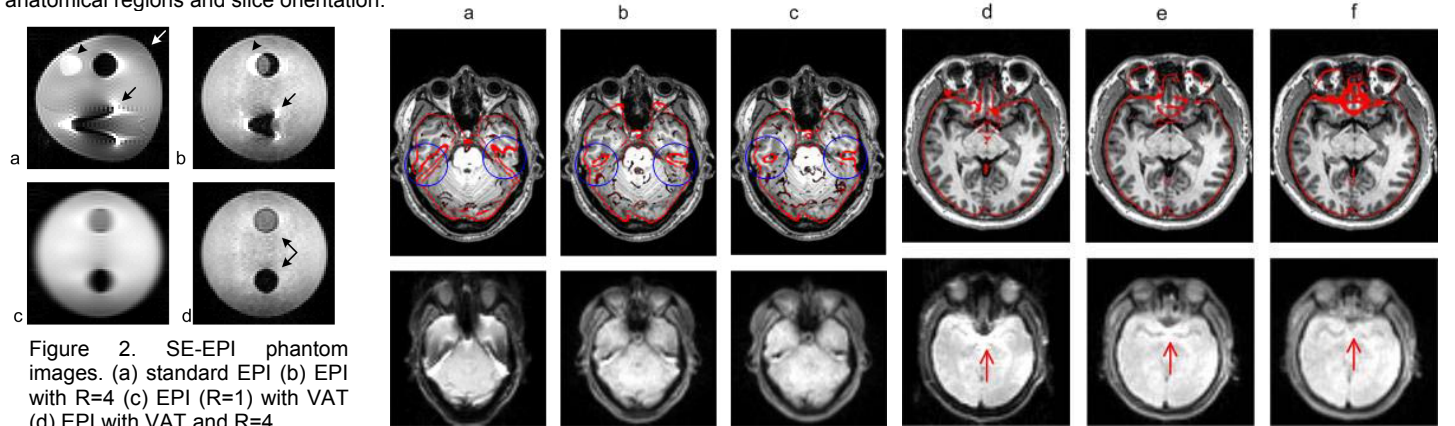


Figure 2. SE-EPI phantom images. (a) standard EPI (b) EPI with R=4 (c) EPI (R=1) with VAT (d) EPI with VAT and R=4

Figure 3. SE-EPI brain images of medial temporal region near ear canal (a-c) and OFC (d-f). (a,d) standard EPI (b,e) EPI with R=4 (c,f) EPI with VAT and R=4

REFERENCES

[1] Med Phys 1988;15(1):7-11. [2] Concepts in Magn Reson 2009;34A(4):238-248.